ResearchGate

See discussions, stats, and author profiles for this publication at: https://www.researchgate.net/publication/233871034

Mineralogical Characterization of Sasol Feed Coals and Corresponding Gasification Ash Constituents

DATASET · DECEMBER 2012

CITATIONS
4

READS
37

4 AUTHORS:

Tivo B. Hlatshwayo
4 PUBLICATIONS **10** CITATIONS
SEE PROFILE

Ratale H. Matjie
North West University South Africa
50 PUBLICATIONS **285** CITATIONS
SEE PROFILE

Zhongsheng Li
The Commonwealth Scientific and Industri…
41 PUBLICATIONS **465** CITATIONS
SEE PROFILE

Colin R. Ward
University of New South Wales
159 PUBLICATIONS **3,078** CITATIONS
SEE PROFILE

Available from: Zhongsheng Li
Retrieved on: 01 February 2016

Mineralogical Characterization of Sasol Feed Coals and Corresponding Gasification Ash Constituents

Tivo B. Hlatshwayo,*,† Ratale H. Matjie,† Zhongsheng Li,‡ and Colin R. Ward‡

Sasol Technology (Proprietary) Limited, Post Office Box 1, Sasolburg, Free State 1947, South Africa, and School of Biological, Earth and Environmental Sciences, University of New South Wales, Sydney, New South Wales 2052, Australia

Received December 11, 2008. Revised Manuscript Received March 3, 2009

Feed coal and coarse ash particles (heated rock fragments and clinkers), produced from Sasol-Lurgi gasifier tests under different operating conditions, have been characterized by quantitative X-ray diffraction, electron microprobe analysis, and associated chemical techniques, as a basis for better understanding of the relations between the mineralogical and physical properties of the ash particles. Crystalline phases in the ashes include quartz particles inherited directly from the feed coal, as well as anorthite, mullite, and diopside, derived from solid-state reactions or crystallization of a silicate melt during the gasification process. Glass, cooled from the melt, is also abundant in the ash materials. The abundance of large particles of hard minerals in the coal or the ash, such as quartz, anorthite, pyrite, and diopside, has been correlated with a laboratory-determined abrasion index and may contribute significantly to wear on mechanical equipment during coal- or ash-handling operations.

1. Introduction

Gasification is the conversion of coal into a combustible gas by pyrolysis and other more heterogeneous reactions.[1] The present study is based on the Sasol-Lurgi fixed-bed, dry-bottom gasifier (Figure 1),[2] using a medium-temperature and high-pressure process suitable for gasifying a large variety of coal feedstock types. In the Sasol-Lurgi process, coal is typically gasified at a pressure of 30 bar in the presence of high-pressure steam and oxygen (as gasification agents) to produce a gas suitable for a range of applications. A mixture of coarse and fine ash particles is formed as a byproduct of the gasification process by the interaction of minerals present in the coal and any admixed noncoal (stone) particles at elevated temperatures and pressures.

Physical transformation within entrainment-type combustion and gasification systems can include coalescence of mineral grains with hot reactive char particles, char fragmentation, and partial coalescence of included minerals and fragmentation or fusion of liberated mineral grains.[3] Although solid-state reactions may also be involved,[4] fluxing elements in minerals, such as carbonates, or elements, such as nonmineral Ca, within the macerals of the coal[5] may react with clays and other components at elevated temperatures and pressures to form a melt. Upon cooling, anorthite may crystallize from this melt.[6] In addition, anorthite and mullite may also be formed by solid-state reactions in lignite coal ash.[7−9] In other instances, heated rock fragments may be encapsulated by the melt and form large clinkers, with the cores of the clinkers remaining at a lower temperature state during the gasification process.[10,11]

Quartz and pyrite are abundant constituents of the mineral matter in some coals and are harder than steel; these minerals may therefore be responsible for wear and abrasion of materials during coal use.[12] Papanicolaou et al.[13] suggest that coal ash particles rich in quartz, feldspar, and pyrite contribute significantly to wear on mechanical parts in a boiler. However, ash

* To whom correspondence should be addressed. E-mail: bafana.hlatshwayo@sasol.com.

† Sasol Technology (Pty) Ltd.

‡ University of New South Wales.

(1) Slaghuis, J. H. Volatile material in coal and the role of inherent mineral matter. M.Sc. Thesis, Department of Chemical Engineering, University of Natal, Natal, South Africa, 1989.

(2) Cooperman, J.; Davis, D.; Seymour, W.; Ruckes, W. L. *U. S. Bureau Mines Bull*. **1951**, 498; Ricketts, T. S. J. Inst. *Fuel* **1961**, *34*, 177; Rudolph, P. E. H. Proc. Synth. Pipeline Gas Symp., 4th, Chicago, Illinois, October **1972**; Elgin, D. C., Perks, H. R. Proc. Synth. Pipeline Gas Symp., 6th, Chicago, Illinois, October **1974**; Lurgi Express Information Brochure No. 1018/10.75, **1975**.

(3) Benson, S. A.; Sondreal, E. A.; Hurley, P. J. Status of coal ash behaviour research. *Fuel Process. Technol.* **1995**, *44*, 1–12.

(4) French, D.; Dale, L., Matulis, C.; Saxby, J.; Chatfield, P.; Hurst, H. J. Characterization of mineral transformations in pulverized fuel combustion by dynamic high-temperature X-ray diffraction analyzer. Proceedings of the 18th Pittsburgh International Coal Conference, Newcastle, Australia, 2001; p 7, CD-ROM.

(5) Li, Z.; Ward, C. R.; Gurba, L. W. Occurrence of non-mineral inorganic elements in low-rank coal macerals as shown by electron microprobe element mapping techniques. *Int. J. Coal Geol.* **2007**, *70*, 137–149.

(6) Matjie, R. H.; van Alphen, C.; Pistorius, P. C. Mineralogical characterisation of Secunda gasifier feedstock and coarse ash. *Miner. Eng.* **2006**, *19*, 256–261.

(7) Benson, S. A. Laboratory studies of ash deposit formation during the combustion of Western U.S. coals. Ph.D. Thesis, The Pennsylvania State University, State College, PA, 1987.

(8) Ilic, M.; Cheeseman, C.; Sollars, C.; Knight, J. Mineralogy and microstructure of sintered lignite coal fly ash. *Fuel* **2003**, *82*, 331–336.

(9) Kalmanovitch, D. P.; Sanyal, A.; Williamson, J. Slagging in boiler furnaces—A prediction technique based on high temperature phase equilibria. *Inst. Energy* **1986**, 120–123.

(10) Matjie, R. H.; van Alphen, C. Mineralogical features of size and density fractions in Sasol coal gasification ash, South Africa and potential by-products. *Fuel* **2008**, *87*, 1439–1445.

(11) Matjie, R. H.; Li, Z.; Ward, C. R.; French, D. Chemical composition of glass and crystalline phases in coarse coal gasification ash. *Fuel* **2008**, *87*, 857–869.

(12) Wells, J. J.; Wigley, F.; Foster, D. J.; Gibb, W. H.; Williamson, J. The relationship between excluded mineral matter and the abrasion index of coal. *Fuel* **2004**, *83*, 359–364.

(13) Papanicolaou, C.; Kotis, T.; Foscolos, A.; Goodarzi, F. Coals of Greece: A review of properties, uses and future perspectives. *Coal Geol.* **2004**, *58*, 147–169.

10.1021/ef8010806 CCC: $40.75 © 2009 American Chemical Society
Published on Web 04/29/2009

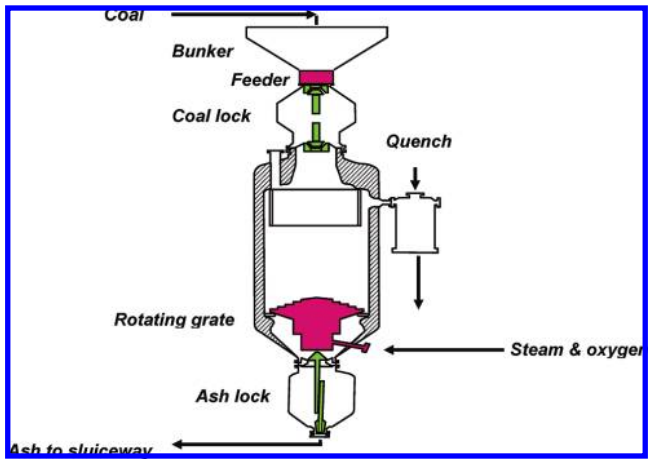

Figure 1. Schematic representation of the Sasol-Lurgi fixed-bed, dry-bottom gasifier.[2]

particles that are rich in relatively soft minerals, such as gypsum, anhydrite, and other minerals with a hardness of less than 3 (Moh's scale),[14] do not seem to contribute to wear on the mechanical parts of the system.

The physical properties of the ash, such as hardness and abrasiveness, as well as particle size, are functions of the mineral matter in the feed coal and the operating conditions of the gasification process. The steam/oxygen ratio controls the maximum operating temperature inside the gasifier as well as the quality and mixtures of the raw gas produced.[15] This paper outlines the mineralogical, physical, and chemical properties of typical coal and ash particles produced during gasifier tests at different operating temperatures. Ash constituents with potentially high abrasion characteristics that could be accountable for wear in mechanical parts of the ash-handling systems were included in the evaluation.

2. Materials and Methods

Samples of coal and corresponding bulk gasification ash (coarse and fine particles) were taken from three commercial gasifier tests (identified as A, B, and C) for mineralogical, physical, and chemical analysis. The ratio of steam/oxygen in the tests was varied to operate at three different temperature conditions in the region of 900−1350 °C, namely, low, medium, and high temperatures. This was performed to determine the effects of temperature on the properties of the ash particles produced.

A representative sample of bulk ash was collected from the gasifier ash lock during each test. The bulk ash sample was split to produce a representative sample that was crushed to 100% passing 1 mm. A number of clinkers and heated rock fragments (stones) were also selected from the remaining bulk gasification ash in each case, and a composite sample of each was made up to investigate more fully some of the mineralogical transformations associated with the different particles in the materials formed during gasification. A representative sample of the feed coal was also collected, along with a number of relatively clean (carbon-rich) coal particles and unheated rock fragments (stone particles) hand-picked from the feed, to further evaluate the different coal components. The coal, stone, ash, and clinker particles were separately crushed to obtain suitable samples for analysis. Those from the low-temperature test were identified as series A; those from the medium-temperature test were identified as series B; and those from the high-temperature test were identified as series C.

2.1. Sample Collection. The gasifier test was performed at each of the selected temperatures (low, medium, and high temperatures) for a period of 4 h or until the gasifier was stable in terms of performance. The gas loads were variable depending upon plant demand, but this was not a factor affecting the test. For ash sampling, the ash lock was first emptied and then pressurized with steam to reach the gasifier pressure of 30 bar. The ash was then released from the gasifier into the ash lock by carefully controlling the speed of the rotating ash grate. The ash was sampled from the ash lock by using a chute that had previously been installed in the test gasifier.

Each sample taken from the ash lock was transferred into three 200 kg drums, to ensure that a representative sample was obtained. The same sampling procedure was followed for all three tests. Samples of the feed coal were taken from the conveyer belts feeding to the coal bunker. The coal samples, bulk gasification ash and individual ash, stone, and clinker particles were crushed (100% passing 1 mm) and subjected to chemical and mineralogical analyses. Anorthite-rich particles were hand-picked from the representative ash sample in all of the tests to make up a composite amount required for the abrasiveness test.

2.2. Proximate and Ultimate Analyses. The coal and ash particles from the gasifier tests were ground to obtain 100% passing 212 μm. The ground samples were subjected to proximate analysis using standard methods to measure the percentages of moisture [South African Bureau of Standards (SABS) 924 and International Organization for Standardization (ISO) 589], ash (ISO 1171), and volatile matter (ISO 562). Ultimate analysis of the samples (C, H, and N) was carried out using the American Society for Testing and Materials (ASTM) D 5373 procedure, and the ASTM D 4239 method was used to determine the total sulfur content.

2.3. X-ray Diffraction (XRD) Analysis. Representative portions of each coal and unheated noncoal (stone) samples were finely powdered and subjected to low-temperature oxygen−plasma ashing using an IPC four-chamber asher, as outlined in Australian Standard 1038, Part 22. The mass percentage of low-temperature ash (LTA) was determined in each case. Representative portions of the LTA from each coal and unheated rock sample, as well as the homogenized (pulverized bulk gasification ash, 100% passing 1 mm) ash, clinker, and heated rock fragments, finely powdered where necessary, were analyzed by XRD using a Phillips X'pert diffractometer with Cu Kα radiation.

Quantitative analyses of mineral phases in each LTA and ash/stone/clinker sample were made using Siroquant, commercial interpretation software initially developed by Commonwealth Scientific and Industrial Research Organisation (CSIRO). Energy Technology[16] based on the Rietveld XRD analysis technique. For the ash, heated stone, and clinker samples, the XRD analysis procedure included an additional evaluation after spiking each powdered material with a known proportion of crystalline zinc oxide, as described by Ward and French,[17] to determine the proportion of amorphous or glassy material as well as the crystalline components.

2.4. X-ray Fluorescence Analysis. A representative portion of each powdered coal sample was ashed at 815 °C. The ash of those samples, as well as representative samples of each homogenized ash, stone, and clinker, dried at 105 °C, was then calcined at 1050 °C, fused with lithium metaborate, and cast into a glass disk following the procedure of Norrish and Hutton.[18] The major elements in the fused disks were analyzed by X-ray fluorescence

(14) Deer, W. A.; Howie, R. A.; Zussman, J. *An Introduction to the Rock-Forming Minerals*, 2nd ed.; Longman Scientific and Technical: Harlow, Essex, U.K., 1992; p 696.

(15) Hlatshwayo, T. B.; Mangena, S. J.; Matjie, R. H.; Jooste, B. Investigation of the Influence of Mineral Composition on the abrasiveness of coal gasification ash. Proceedings of the 24th Pittsburgh International Coal Conference, Johannesburg, South Africa, Sept 10−14, 2007; paper *43-1*, p 12, CD publication.

(16) Taylor, J. C. Computer programs for standardless quantitative analysis of minerals using the full powder diffraction profile. *Powder Diffr.* **1991**, *6*, 2–9.

(17) Ward, C. R.; French, D. Determination of glass content and estimation of glass composition in fly ash using quantitative X-ray diffractometry. *Fuel* **2006**, *85*, 2268–2277.

(18) Norrish, K.; Hutton, J. T. An accurate X-ray spectrographic method for the analysis of a wide range of geological samples. *Geochim. Cosmochim. Acta* **1969**, *33*, 431–453.

Table 1. Proximate and Ultimate Analyses for Representative Feed Coal and Gasification Ash Samples Reported on an Air-Dry Basis

	coal A	coal B	coal C	ash A	ash B	ash C
Proximate Analysis (wt %)						
inherent moisture	3.8	3.8	4.0	0.3	0.2	0.1
ash	32.8	29.1	25.8	93.8	94.4	95.3
volatile matter	20.6	22.3	22.1	1.3	1.2	0.9
fixed carbon	42.8	44.8	48.1	4.6	4.2	3.7
Ultimate Analysis (wt %)						
carbon	50.45	53.31	56.20	5.74	5.26	4.36
hydrogen	2.54	2.81	2.83	0.13	0.10	0.09
nitrogen	1.27	1.35	1.44	0.08	0.09	0.06
total sulfur	1.17	0.96	0.76	0.34	0.30	0.31

spectrometry (XRF) using a Philips PW 2400 spectrometer and SuperQ software.

2.5. Electron Microprobe Analysis. Hand-picked lump samples of ash, heated stone, and clinker samples were mounted into polished sections and carbon-coated for electron microprobe analysis. Points on individual components in the samples were analyzed using a Cameca SX-50 electron microprobe equipped with the Windows-based SAMx operating system and interface software. The accelerating voltage for the electron beam was 15 kV, and the filament current was 20 nA, with a beam spot size on the sample of around 1−5 μm in diameter. Calibration from relevant standards supplied with the instrument was carried out for each of the elements analyzed. Backscattered electron (BSE) images of representative parts of each sample were also collected, to indicate the mode of occurrence of the various components.

2.6. Abrasiveness Index. The total mass loss [expressed in milligrams of iron (mg of Fe)] sustained by four carbon steel blades when rotated for a fixed number of revolutions in a specified charge of coal is taken as a measure of the abrasiveness of the coal and is called the index of abrasion. Representative samples of coal and ash material (about 4.0 kg, sized to less than 5 mm) were placed in a pot, and four carbon steel plates with defined dimensions and Vickers hardness were fixed to the rotating arms of a quadrant for determination of the abrasiveness index. The plates were carefully adjusted to a specified distance from the walls of the pot, and the arms were rotated for 8 min at 1500 rpm.[19,20] The abrasion index of each sample was expressed as the total milligrams of metal abraded from the carbon steel blades per unit mass of sample material used. In this study, the abrasiveness index test was performed in duplicate and the average value of abrasiveness index was reported.

3. Analytical Results

3.1. Proximate and Ultimate Analyses. The results of proximate and ultimate analyses for the six samples, expressed on an air-dried basis, are given in Table 1. The coals have around 4% moisture and ash yields of between 25 and 32%, with total sulfur between 0.7 and 1.2%. The ash samples contain up to 5% unburned carbon and around 0.3% total sulfur and have very low (<0.5%) moisture contents.

3.2. Mineral Matter in Feed Coal. Table 2 summarizes the percentages of the individual minerals in the LTA of representative feed coal and unheated stone samples based on the powder XRD and Siroquant evaluation. The LTA derived from the two feed coals analyzed was made up mainly of kaolinite (a little over 50%), with lesser proportions of quartz, illite and interstratified illite/smectite, mica, calcite, dolomite, and pyrite and minor proportions of anatase and/or rutile. A small proportion (around 5%) of bassanite ($CaSO_4 \cdot {}^1/_2H_2O$) was also found in the LTA samples of the feed coal; this was probably derived from interaction of the organically associated calcium in the coal with organic sulfur during the low-temperature ashing process. Similar mineralogy is noted for other South African coals.[21]

Table 2. Mineralogical Analysis of Feed Coal and Coal Stone Samples

sample	coal B1 homogenized	coal C1 homogenized	coal C1 carbon-rich	coal C1 stones
LTA (wt %)	32.7	31.3	22.4	92.5
LTA Mineralogy (wt %)				
quartz	19.7	17.8	16.7	35.4
kaolinite	51.7	53.9	49.7	56.2
illite	3.9	5.4		2.4
illite/smectite	1.3	0.3		
mica	4.1	1.5		4.4
calcite	1.3	2.5	4.0	
dolomite	7.7	10.7	21.2	
pyrite	4.1	2.1	2.3	0.2
anatase	0.7			0.1
rutile		0.8		1.3
bassanite	5.4	4.9	6.1	

Table 3. Chemical Composition of Feed Coal Ash (815 °C) and Coal Stone Samples (wt %), Determined by XRF Analysis

sample	coal B1 homogenized	coal C1 homogenized	coal C1 carbon-rich	coal C1 stones
SiO_2	48.41	49.07	42.93	58.05
Al_2O_3	24.68	24.46	22.81	21.07
Fe_2O_3	6.83	4.58	4.07	1.56
MnO	0.05	0.05	0.08	0.01
CaO	7.04	8.44	13.64	0.07
MgO	2.24	2.76	5.23	0.03
Na_2O	0.34	0.38	0.40	1.43
K_2O	0.65	0.58	0.22	1.11
TiO_2	1.38	1.36	1.17	0.99
P_2O_5	0.58	0.46	0.69	0.18
SO_3	4.30	4.59	5.59	0.21
LOI	3.52[a]	3.28[a]	3.17[a]	15.5
total	100	100	100	100.21

[a] Loss on ignition (LOI) estimated by difference.

The carbon-rich coal sample from test C had a similar mineral assemblage to the homogenized (pulverized 100% passing 1 mm) feed coal but with a lower LTA percentage, higher proportions of dolomite and calcite, slightly more bassanite, and no detectable illite, illite/smectite, anatase, or rutile. The LTA of the unheated stone sample from test C contained significantly higher proportions of quartz than the LTA of either the feed coal or the carbon-rich material, similar proportions of kaolinite, illite, mica, and rutile, a very low percentage of pyrite, and no detectable dolomite, calcite, or bassanite.

Chemical analysis of the feed coal materials, ashed at 815 °C (Table 3), indicates a little under 50% SiO_2 and 25% Al_2O_3 for the homogenized feed coals, with lesser proportions of Fe_2O_3, CaO, MgO, and TiO_2. The proportion of sulfur retained in the laboratory ash, expressed as SO_3, was around 4.5%. The loss on ignition for these ashes, estimated by difference because of the small sample size and probably mainly representing traces of unburned carbon, is indicated at around 3%.

The carbon-rich coal sample has slightly lower proportions of SiO_2 and Al_2O_3 relative to the homogenized materials, similar proportions of Fe_2O_3 and TiO_2, and higher proportions of CaO, MgO, and SO_3. These are consistent with the increased

(19) Daly, M. J. Determination of the index of abrasion of coal—Test procedure. ESKOM, 1993.

(20) Yancey, H. F.; Geer, M. R.; Price, J. D. An investigation of the abrasiveness of coal and its associated impurities. Mining Engineering, 1951; BS1016-111:1998.

(21) Pinetown, K. L.; Ward, C. R.; van der Westhuizen, W. A. Quantitative evaluation of minerals in coal deposits in the Witbank and Highveld Coalfields and the potential impact on acid mine drainage. *Int. J. Coal Geol.* **2007**, *70*, 166–183.

Table 4. Chemical Composition of Ash, Clinker, and Heated Stone Samples (wt %), Determined by XRF Analysis

sample	ash A1 homogenized	ash B1 homogenized	ash C1 homogenized	ash A1 clinker	ash B1 clinker	ash C1 clinker	ash A1 stones	ash B1 stones	ash C1 stones
SiO_2	51.3	50.5	52.0	55.6	49.0	57.1	51.4	64.0	54.9
Al_2O_3	23.1	24.0	23.9	22.5	24.4	26.5	31.8	21.6	32.0
Fe_2O_3	5.9	6.2	6.0	8.0	8.6	5.1	1.6	4.7	5.7
MnO	0.06	0.06	0.06	0.06	0.07	0.06	0.02	0.02	0.04
CaO	8.1	8.2	8.9	9.0	9.8	7.0	0.23	1.53	0.80
MgO	1.82	2.10	2.07	2.41	2.64	2.04	0.05	0.10	0.39
Na_2O	Bld[a]	0.13	0.33	0.01	0.01	Bld[a]	0.70	0.30	Bld[a]
K_2O	0.64	0.54	0.61	0.86	0.39	0.60	1.10	1.79	1.64
TiO_2	1.46	1.53	1.48	1.60	1.55	1.41	1.94	0.98	1.67
P_2O_5	0.55	0.64	0.59	0.62	0.55	0.39	0.19	0.10	0.15
SO_3	0.11	0.08	0.13	0.30	1.04	0.17	0.01	0.35	0.20
LOI	6.78	6.50	5.13	0.29	1.67	0.35	12.27	5.18	3.04
total	99.80	100.55	101.20	101.27	99.80	100.66	101.36	100.59	100.47

[a] Bld = below limit of detection.

Table 5. Chemical Composition (wt %) of Homogenized Coal Ash (815 °C) and Gasifier Ash Samples, Normalized to an SO_3 and LOI Free Basis

sample	coal B1 homogenized	coal C1 homogenized	ash A1 homogenized	ash B1 homogenized	ash C1 homogenized
SiO_2	52.5	53.3	55.2	53.7	54.2
Al_2O_3	26.8	26.6	24.9	25.6	24.9
Fe_2O_3	7.4	5.0	6.4	6.6	6.2
MnO	0.05	0.05	0.06	0.06	0.06
CaO	7.6	9.2	8.7	8.8	9.3
MgO	2.43	3.00	1.96	2.23	2.16
Na_2O	0.37	0.41	0.00	0.14	0.34
K_2O	0.71	0.63	0.69	0.57	0.64
TiO_2	1.50	1.48	1.57	1.63	1.54
P_2O_5	0.63	0.50	0.59	0.68	0.61
total	100.00	100.00	100.00	100.00	100.00

Table 6. Mineralogy of Ash, Clinker, and Heated Stone Samples (wt %) by XRD Analysis and Siroquant

sample	ash A1 homogenized	ash B1 homogenized	ash C1 homogenized	ash A1 clinker	ash B1 clinker	ash C1 clinker	ash A1 stones	ash B1 stones	ash C1 stones
quartz	12.9	11.8	9.8	7.9	6.5	8.3	24.1	46.5	14.9
anorthite	11.6	13.2	14.8	33.5	47.7	27.7			
mullite	23.0	23.7	18.0	6.5	8.7	14.5	35.2	17.2	43.1
cristobalite	2.7	1.4	3.4	5.7		7.5	0.2	0.1	0.2
diopside	1.9	3.1	2.7	4.6	5.0	1.8		1.7	1.9
anatase							1.3		0.7
rutile							0.9	2.7	2.3
amorphous	47.9	46.9	51.3	41.8	32.2	40.3	38.1	31.8	37.0

proportions of calcite and dolomite observed from the XRD data (Table 2). The additional Ca derived from these minerals was also probably responsible for further retention of S (as SO_3) in the laboratory ash material. The ash of the carbon-rich coal has lesser proportions of K_2O than the homogenized feed material, consistent with the lesser proportions of illite and mica indicated by the XRD data.

The ash of the stone sample from the feed coal has a higher proportion of SiO_2 and a lower proportion of Al_2O_3 than the other materials, consistent with the higher quartz content in mineralogy. It also has lower proportions of Fe_2O_3, CaO, MgO, and P_2O_5 and a lower percentage of retained SO_3. The proportions of K_2O and Na_2O are both higher than for the coal samples. The increased K_2O may in part reflect a greater abundance of illite and/or mica, but the increased proportions of these minerals indicated by XRD cannot explain all of the difference observed. Feldspar minerals, if present, might possibly explain such increased proportions of Na_2O and K_2O, but no indication of feldspar minerals was found in the XRD pattern of the coal stone sample.

3.3. Chemistry and Mineralogy of Ash, Clinker, and Heated Stone Samples. The chemical composition of the homogenized ash, clinker, and heated stone samples, expressed as percentages of the major element oxides, are given in Table 4. The ash samples from the gasifier have much lower proportions of SO_3 than the laboratory ashes of the coal samples (Table 3). The difference may reflect the higher temperatures associated with the gasification process, which would be expected to break down any sulfur-bearing minerals (calcium sulfates and pyrite) and convert more of the sulfur to volatile forms.[11]

The analyses of the laboratory ashes of the homogenized coals (Table 3) and the homogenized gasifier ash samples (Table 4) have been recalculated in Table 5 to express the data on a SO_3 and loss on ignition (LOI) free basis, eliminating the impact of retained sulfur and unburnt carbon on the relative abundance of the main ash-forming constituents. Table 5 shows that the proportions of the major elements in the homogenized gasifier ashes (B1 and C1) are very similar to those of the same elements in the corresponding homogenized feed coals. There is a possible suggestion that the gasifier ashes, expressed on this basis, have slightly more SiO_2 and slightly less Al_2O_3 than the laboratory ashes of the corresponding feed coals, but in view of the different nature of the sample sets, this is not necessarily significant.

Although the individual results are more variable, the clinkers in the test series have a similar chemical composition to the homogenized ashes (Table 4). Clinker B1 shows some slight

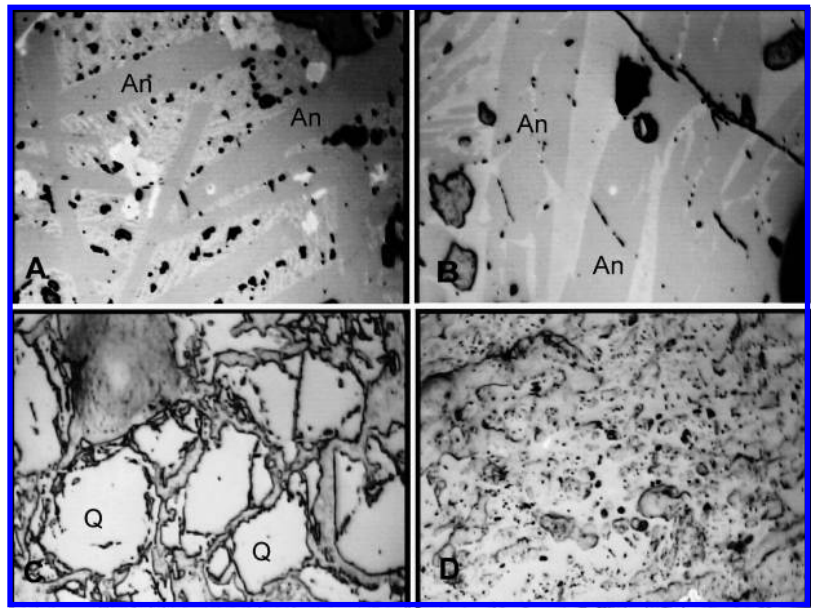

Figure 2. Backscattered electron images showing the mode of occurrence of key minerals in the ash samples: (A) anorthite (An) with interstitial vesicular and microcrystalline glassy groundmass, ash A1, homogenized; (B) anorthite (An) with interstitial glass and some angular quartz particles (lower left), ash A1, clinker; (C) angular quartz grains (Q) apparently intact after heating, ash A1, clinker; and (D) fine particles of metakaolin in a glassy matrix, ash A1, clinker. Field of view: images A−C, 300 μm; image D, 100 μm.

Table 7. Chemical Composition of Minerals in Selected Ashes (wt %) as Indicated by Electron Microprobe Analysis

elements	O	Na	Mg	Al	Si	P	S	K	Ca	Ti	Mn	Fe
ash C1, homo,[a] anorthite	45.18	0.42	0.44	17.16	20.62	0.17	0.03	0.18	12.55	0.15	0.02	1.37
ash C1, homo,[a] metakaolin	46.90	0.16	0.15	22.23	22.95	0.02	0.01	0.88	0.03	0.34	0.01	0.86
ash C1, homo,[a] glass	43.73	0.25	1.32	11.18	24.69	0.40	0.04	1.78	2.52	0.76	0.04	5.27
ash C1, homo,[a] TiO_2	41.92	0.01	0.02	2.34	1.41	0.21	0.01	0.06	0.14	55.41	0.01	1.99
ash C1, homo,[a] quartz	51.60	0.01	0.00	0.02	45.23	0.01	0.01	0.01	0.00	0.02	0.01	0.03
ash C1, clinker, anorthite	45.09	0.36	0.12	18.77	20.03	0.04	0.01	0.05	12.77	0.07	0.01	0.34
ash C1, clinker, metakaolin	45.36	0.31	1.19	17.76	20.97	0.49	0.02	1.97	3.04	1.48	0.05	3.49
ash C1, clinker, glass	42.99	0.29	1.50	14.90	18.80	0.41	0.04	1.55	6.84	2.20	0.06	4.91
ash C1, stone, metakaolin	47.76	0.18	0.31	22.07	23.37	0.01	0.01	2.31	0.04	0.62	0.02	0.68
ash C1, stone, glass	46.68	0.33	0.16	8.28	31.92	0.02	0.00	6.52	1.58	0.49	0.07	0.91
ash C1, stone, quartz	52.64	0.00	0.00	0.01	46.16	0.01	0.01	0.01	0.01	0.01	0.01	0.01
coal C1, stone, illite	41.88	0.48	0.58	17.34	20.48	0.00	0.01	7.51	0.00	0.33	0.02	1.88
coal C1, stone, kaolinite	42.66	0.69	0.09	18.59	22.18	0.01	0.05	0.16	0.04	0.15	0.01	0.79
coal C1, quartz	52.66	0.00	0.00	0.00	46.17	0.01	0.00	0.01	0.01	0.01	0.03	0.07

[a] Ash C1, homo = homogenized ash C1 sample.

differences, but these probably reflect the higher proportions of SO_3 and LOI associated with this particular sample. The heated stones, however, have much lower proportions of CaO and MgO and, in some cases, also Fe_2O_3, offset by higher percentages of SiO_2, Al_2O_3, and/or SO_3, and higher LOI values. This is consistent with the differences in chemical composition noted for the unheated stone sample in Table 3, relative to the homogenized feed coal materials.

Table 6, derived from the results of XRD analysis and Siroquant, shows that all of the ash, clinker, and stone samples contain significant proportions of quartz and mullite and, in most cases, minor proportions of diopside ($CaMgSi_2O_6$). The homogenized ash and clinker samples also contain anorthite ($CaAl_2Si_2O_5$) and, in most cases, cristobalite (a high-temperature form of SiO_2), but neither of these minerals is found in significant concentrations in the heated stone materials. The heated stones also contain rutile and, in some cases, anatase. Despite similar TiO_2 concentrations (Table 4), neither anatase nor rutile could be identified in the ash or clinker samples.

The bulk of the ash, clinker, and heated stone samples are represented by amorphous material. The amorphous content of the homogenized ashes is slightly higher than that of the clinker or stone samples. Although the differences are not large, Table 6 also suggests that the proportion of anorthite in the homogenized ash increases and those of quartz and mullite decrease with increases in the temperature of the gasification tests. This may reflect formation of anorthite by solid-state reactions between quartz, mullite, and Ca-bearing glass as temperature increases or possibly melting of the glass followed by crystallization of anorthite upon cooling.[11] The heated stones have higher percentages of quartz and mullite than the ashes and clinkers, while the clinkers contain higher proportions of anorthite and lower proportions of quartz and mullite than the homogenized ash materials, again possibly because of melting followed by anorthite crystallization.

3.4. Data from Electron Microprobe Studies. Parts A and B of Figure 2 show the mode of occurrence of anorthite, quartz, and metakaolin in the ash samples, as observed from backscattered electron images captured during electron microprobe analysis of polished sections. The anorthite typically forms lath-like euhedral crystals, with a typical size range of 20−50 μm (width) × 100−500 μm (length), set in a groundmass of microcrystalline and sometimes vesicular glassy material. Analysis under the microprobe (Table 7) indicates a composition corresponding approximately to that of stoichiometric An_{95} (Ca = 13.72%, Al = 18.97%, Si = 20.75%, O = 46.14%, and Na = 0.41%). Only very minor proportions (<0.5%) of Na and K

Table 8. Hardness of Minerals Present in Coal and Gasification Ash Samples Based on Moh's Scale[14]

mineral	composition	hardness
quartz	SiO_2	7
cristobalite	SiO_2	6.5
pyrite	FeS_2	6.3
anorthite	$CaAl_2Si_2O_8$	6.3
rutile	TiO_2	6.2
diopside	$CaMgSi_2O_6$	6
anatase	TiO_2	5.8
dolomite	$CaMg(CO_3)_2$	3.5
calcite	$CaCO_3$	3
kaolinite	$Al_2Si_2O_5(OH)_4$	2.3
illite	$KAl_4[Si_7AlO_{20}](OH)_4$	1.5
mullite	$Al_6Si_2O_{13}$	6−7

are present, but around 1% and, in one sample, around 3% Fe typically occur in the anorthite of the ash samples. Most of the Fe probably occurs as fine inclusions of an iron mineral, such as magnetite, but some may represent incorporation of Fe in place of Ca within the lattice structure.

Backscattered images of quartz in the ash samples (Figure 2C) typically show irregular, broadly equidimensional particles, probably representing unreacted fragments inherited from the coal and noncoal (sandstone, siltstone, and carbonaceous shale) components in the feedstock of the gasification process. The material is close to stoichiometric quartz (46.67% Si and 53.33% O) in composition (Table 7).

Metakaolin, with a somewhat variable chemical composition, occurs as very fine grained irregular particles intimately associated with the glassy groundmass (Figure 2D). Mullite, formed at high temperatures by solid-state reactions from kaolinite and other clay minerals, may also be present along with the metakaolin, as masses of very fine crystals in the glassy groundmass material.

The microprobe study also indicates the presence of an essentially homogeneous aluminosilicate glass with a varying chemical composition. Especially in the ash and clinker samples, this glass typically has around 20−25% Si, 10−15% Al, 2−12% Ca, and 1−4% Mg, along with minor proportions of Fe and Ti. The glass may, however, also contain fine crystalline or cryptocrystalline phases (such as tiny metakaolin particles), too small for separate identification or analysis by the microprobe system.

Other phases identified under the microprobe include small particles consisting almost entirely of Ti and/or Fe oxide material. These may be remnants of anatase or rutile from the feed coal or the associated noncoal components.

4. Formation of Minerals in Ash and Clinker Samples

The mullite, anorthite, diopside, and cristobalite in the ash samples were probably derived from the mineral transformation at elevated temperatures and pressures during gasification. Cristobalite and mullite are high-temperature transformation products of clay minerals, such as kaolinite, and cristobalite may represent a phase change, resulting from the cracking of quartz particles at temperatures above 870 °C.[11]

Formation of anorthite in the gasification process may start with solid-state reactions at around 900 °C and persists to temperatures of above 1200 °C, with no significant change in the crystal structure until anorthite decomposition takes place at temperatures above 1400 °C.[6] The interaction of kaolinite at high temperatures with dolomite and/or calcite may also result in the formation of an aluminosilicate melt. Upon cooling as the ash mixes with steam and oxygen in the lower temperature regions of the gasifier, anorthite and to a lesser extent mullite begin to crystallize out from this melt.[6]

Macroscopically, the coarse ash consists of rock fragments (heated stones) set in a black/gray glassy matrix. As indicated above, the matrix contains distinct elongated crystalline laths of anorthite[10,11] (parts A and B of Figure 2).

Because the overall proportion of CaO in the homogenized ashes and the clinker samples is essentially the same, the higher proportion of anorthite and lower proportions of quartz and mullite in the clinker samples (Table 6) may indicate that the clinkers were subjected to higher temperatures within the gasification system. Alternatively, they may have cooled more slowly during passage through the system, allowing more time for anorthite crystallization to take place. The second possibility is also consistent with the lower proportion of amorphous material (glass) in the clinker samples.

The proportion of quartz in the homogenized ashes of the present study is slightly lower than that in the LTA of the homogenized feed coals (Table 2). Similar studies[17] indicate that the quartz in coal feedstocks can pass essentially unaltered into the fly ash of pulverized fuel power stations. A comparison of Tables 2 and 6, however, suggests that some of the quartz in the coals of the present study was transformed into cristobalite, incorporated into the amorphous phase by melting, or consumed by reactions leading to the formation of the anorthite components. Similar comparisons between the quartz content of the heated stones and that of the unheated stone sample in Table 2 were not attempted, because of the inherently variable nature of the individual particles involved.

5. Mineralogy and Ash Abrasiveness

Table 8 lists the relative hardness of the mineral phases occurring in the coal, stone, ash, and clinker samples of the present study. The hardness in this case is derived from Moh's scale,[14] within which a carbon steel has a hardness value of around 6. A number of minerals in the coal and ash samples have hardness values greater than or equal to 6, and if present as coarse particles, these extraneous minerals could contribute significantly to wear of steel mechanical parts of an ash-handling system. It is acknowledged that abrasion is a complex function of the physical properties of the particles involved, including

Table 9. Average Value of Abrasiveness Index and Proportion of Coarse Minerals (wt %) with Moh Hardness of 6 or More in Coal and Ash Samples

sample	feed coal (C1)	coal stone	ash (homogenized)	ash stone	clinkers	anorthite-rich fraction
average value of abrasiveness index	217	4569	5520	3441	4881	6168
quartz	3.7	32.7	9.8	14.9	8.3	
cristobalite			3.4	0.2	7.5	
pyrite	0.5	0.2				
anorthite			14.8		27.7	
rutile						
diopside			2.7	1.9	1.8	
total hard minerals	4.3	32.9	30.7	17.0	45.3	

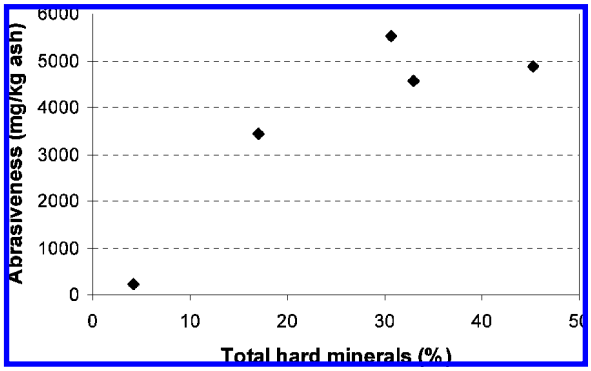

Figure 3. Mineralogy of feed coals and ashes from Sasol-Lurgi gasifiers in relation to abrasiveness characteristics.

size, shape, and hardness, presenting a challenge in relating these properties mathematically.

The abrasion index test results for the coal and ash samples are presented in Table 9. The percentages of those minerals in the relevant samples with hardness of 6 or above are also provided in Table 9 based on the XRD data (Tables 2 and 7). For the coal and unheated stone samples, where the mineralogy of the LTA is given in Table 2, these were recalculated as percentages of the original unashed materials (i.e., to include also the organic matter). Although mullite has a hardness of between 6 and 7, the mineral was not included in this assessment because of its fine particle size. The total percentages of hard minerals that might potentially be related to the abrasiveness of the samples, as a fraction of the host material, are given in Table 9.

Figure 3 provides a plot of the total percentage of hard minerals in the samples against the abrasiveness index of the samples concerned. Although the number of data points is limited, it shows a trend of increasing abrasiveness with increasing proportion of hard minerals and, as such, indicates the usefulness of quantitative XRD in understanding and predicting the abrasiveness of ash and similar materials in material-handling operations. The abrasion results suggest some relationships that warrant further investigation, as a basis for better understanding of the wear observed in ash-handling systems. It is hoped, however, that the improved understanding of the role of ash mineralogy arising from the present study will enable operators to estimate wear rates to susceptible components and develop appropriate maintenance and refurbishment strategies to deal with particular ash materials.

6. Conclusions

X-ray diffraction using Rietveld-based techniques has been applied to evaluating the percentages of individual minerals, as well as the amorphous or glassy component, in the ash, clinker, and heated but otherwise unaltered particles of noncoal rock ("stones") produced as a byproduct of the Sasol-Lurgi gasification process. This allows for a comparison between the mineralogy of the feed coal and associated noncoal particles supplied to the gasification system. Textural observations under the electron microprobe indicate that quartz particles in the feed coal mainly pass through the gasifier without significant alteration but that clay minerals and carbonates in the coal interact to form mullite and cristobalite and also to form a melt from which anorthite crystallizes as the ash cools. The overall proportion of anorthite in the ash may also increase slightly, and quartz and mullite decrease, with increases in the gasification temperature.

The mullite in the ashes, as well as the material with more variable chemistry representing metakaolin, forms mainly very fine microcrystalline particles. Some of the other minerals, however, especially quartz and anorthite, form relatively large crystals or fragments within the ash. The abundance of hard minerals that form relatively coarse particles, such as quartz, diopside, and anorthite, can be correlated with the degree of abrasion generated during laboratory tests. These components in the ash or, in some cases, in different fragments within the feed coal may contribute significantly to the wear on steel materials in coal- or ash-handling systems. Mineralogical analysis of coal or ash products may therefore be of assistance in identifying sources of excessive abrasion or in predicting the abrasiveness characteristics of particular ashes produced by gasification and related processes. Further work is needed to better define the mathematical relationships between the physical properties of the different minerals contributing to abrasion from coal gasification ash in material-handling systems. It is hoped, however, that the improved understanding of the role of ash mineralogy arising from the present study will enable operators to estimate wear rates to susceptible components and develop appropriate maintenance and refurbishment strategies to deal with particular ash materials.

Acknowledgment. The authors thank the management of Sasol Technology Research and Development for their support and permission to conduct these studies. Assistance provided by Setobane Mangena and Berni Jooste of Sasol and Irene Wainwright, Rad Flossman, and Karen Privat of the University of New South Wales, as well as by the Coal and Minerals Technology Laboratory of the South African Bureau of Standards, is also gratefully acknowledged for carrying out some of the analyses. Thanks are also extended to the reviewers for their constructive comments on the manuscript.

EF8010806